Acta Oceanol. Sin., 2013, Vol. 32, No. 6, P. 6-12
DOI: 10.1007/s13131-013-0319-z
http://www.hyxb.org.cn
E-mail: hyxbe@263.net

Air-sea interactions associated with tropospheric biennial oscillation in South China Sea summer monsoon and their effects on El Niño-Southern Oscillation

ZHENG Bin[1*], LU Feng[1,2], WEI Hongcheng[1,2]

[1] Guangzhou Institute of Tropical and Marine Meteorology, China Meteorological Administration, Guangzhou 510080, China
[2] Nanjing University of Information Science & Technology, Nanjing 210044, China

Received 16 November 2011; accepted 26 September 2012

Abstract
The South China Sea summer monsoon (SCSSM) behaves with prominent climate variability from the intraseasonal to interdecadal time scales. On the interannual time scale, the biennial variability (so-called tropospheric biennial oscillation, TBO) is as important as the El Niño-Southern Oscillation (ENSO) period. Some observed data sets, including reanalysis data, are used to explore the associated air-sea interactive physical processes and how the SCSSM TBO affects the ENSO. The results show that the shearing vorticity induced by the north Indian Ocean sea surface temperature anomalies (SSTAs) and the anomalous Philippine Sea anticyclone both contribute to the TBO in the SCSSM. The results also indicate that the ENSO has a weak effect on the SCSSM TBO, whereas the latter affects the ENSO to some extent.

Key words: South China Sea, monsoon, tropospheric biennial oscillation, El Niño-Southern Oscillation

Citation: Zheng Bin, Lu Feng, Wei Hongcheng. 2013. Air-sea interactions associated with tropospheric biennial oscillation in South China Sea summer monsoon and their effects on El Niño-Southern Oscillation. Acta Oceanologica Sinica, 32(6): 6–12, doi: 10.1007/s13131-013-0319-z

1 Introduction

Monsoons denote significant seasonal variations in winds and precipitation. The South China Sea (SCS) is located on the south of the Mainland of China. It has plenty of rain in boreal summer (June-August) and relatively less precipitation in boreal winter. In September, great rainfall shifts to the equator gradually, and precipitation in the SCS begins to decrease (Figs 1a, b and c). Moreover, SCS winds behave in seasonal switching. In summer, lower SCS winds (850 hPa) change from northeasterly to southwesterly (Figs 1d, e and f), and high-level leaning south winds converse into the northeasterlies (Figs 1g, h and i). SCS winds change direction southwardly starting from September. Similar results can be obtained using different data sets. There exists a typical monsoon in the SCS area, which is independent from the western north Pacific monsoon. Figure 2 shows that boreal summer low-level winds form a trough in the SCS area and an anticyclone over the western north Pacific (WNP). Thus, southwesterly winds prevail in the SCS, whereas southeasterly winds prevail over the WNP, implying a monsoon system in the SCS that is different from the WNP monsoon system.

The outbreak of the SCS summer monsoon (SCSSM) has an important contribution to precipitation in South China. In addition, the Rossby wave excited by the strong convective activity during the SCSSM period can spread to the northeast and form the PJ wave train (Nitta, 1987), thus affecting the summer climate in East Asia (Kurihara, 1989; Huang and Sun, 1992; Lu, 2001). The wave train can even propagate across the Pacific and affect summer rainfall in the US Great Plains (Wang et al., 2001). The SCS connecting the South Asia monsoon, the East Asia monsoon, and the WNP monsoon has a very unique location. The SCSSM is a subsystem, which breaks out relatively earlier among Asian summer monsoons. Tao and Chen (1987) initially believed that the SCSSM is the first onset among the Asian summer monsoons. With detailed studies, particularly the SCS monsoon experiment (Lau et al., 2000; Ding et al., 2004), it has been found that the Asian summer monsoon first breaks out in the eastern Bay of Bengal-Indochina, followed by the SCSSM and the WNP monsoon (Wang and Lin, 2002). The SCSSM and the WNP monsoon (Li and Wang, 2005) are significant on the seasonal scale to interdecadal time scales (Wang et al., 2009; Zheng et al., 2009). Specifically, the significance of SCSSM on the quasi-biennial scale is secondary to its 4 a El Niño-Southern Oscillation (ENSO) period (Zheng et al., 2009). The quasi-biennial oscillation of SCSSM is not studied in depth and is generally attributed to the ENSO. Equatorial western Pacific westerly anomalies form cyclonic anomalies in the SCS, thus strengthening the SCSSM in the year when the El Niño develops. In the following autumn, the Philippines anticyclone is established quickly (Wang and Zhang, 2002) and is maintained from winter to early summer in the next year (Wang et al., 2000). Thus, it can be said that the existence of anticyclone weakens the SCSSM. However, there are positive SSTAs in the SCS after the El Niño events (Wang et al., 2002; Wang et al., 2006), and inducing more latent-heat flux in the SCS (Zeng et al., 2009) would enhance the SCSSM since the active SCCCM is clearly correlated with the positive and negative phases of the intraseasonal variability of latent-heat flux in the SCS (Zeng and Wang, 2009). The aim of the current work is to further understand the interac-

Foundation item: The Major State Basic Research Development Program (973 Program) of China under contract No. 2011CB403403).
*Corresponding author, E-mail: zbin@grmc.gov.cn

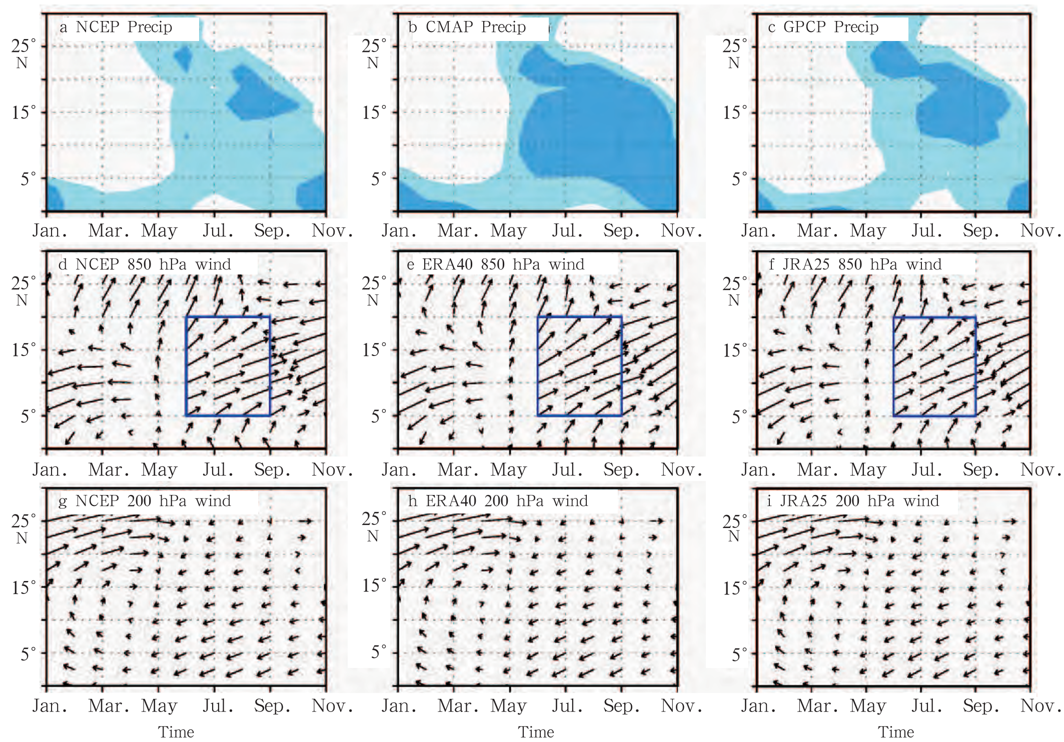

Fig.1. 105°–120°E averaged climatological precipitation (mm/d) (a, b and c), (d-f) 850 hPa winds (m/s) (d, e and f) and 200 hPa winds (m/s) (g, h and i). The shaded area in Figs 1a, b and c denote the region wherein mean precipitation is more than 6 mm/d.

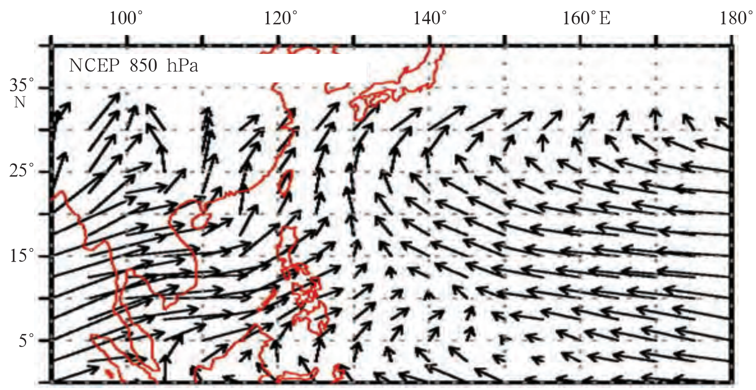

Fig.2. NCEP/NCAR June-August mean 850 hPa winds.

tion between the ENSO and the tropospheric biennial oscillation (TBO) as well as the possible causes of the TBO in the SCSSM.

The data used in this paper include the monthly data of the surface and 200 hPa winds, latent heat, and shortwave radiation of the National Centers for Environmental Prediction (NCEP)/National Center for Atmospheric Research (NCAR) reanalysis data (Kalnay et al., 1996). The 200 hPa wind is on a grid of 2.5° latitude by 2.5° longitude, while the rest are on a gauss grid. The precipitation reconstruction data set (Chen et al., 2002) is likewise on a grid of 2.5° latitude by 2.5° longitude. Extended reconstructed sea surface temperature version 3 (ERSST.v3) monthly sea surface temperature data are on a grid of 2° latitude by 2° longitude (Smith et al., 2008). Monthly thermocline layer data based on the simple ocean data assimilation (SODA) (Carton et al., 2000a, b) is on a gauss grid. Except the SODA data from January 1968 to December 2001, the rest of the data span from January 1968 to December 2009.

2 Defining SCS summer monsoon (SCSSM) intensity

SCSSM is a large-scale system with easterly vertical shear as well as significant seasonal changes in rainfall and low- and high-level winds. Thus, the area (5°–20°N, 105°–120°E, see boxes in Figs 1d, e and f) was selected in this work to denote an SCSSM region where there are evident seasonal changes in rainfall and winds, with simultaneous, low-level prevailing southwesterly and high-level strong northeasterly winds. Accordingly, average precipitation in the area, with climatology removed, is defined as the index of SCSSM intensity. NCEP precipitation has longer time series, and the index of SCSSM intensity is established on the basis of the dataset. Figure 3 shows similar interannual variability although the NCEP precipitation has less magnitude

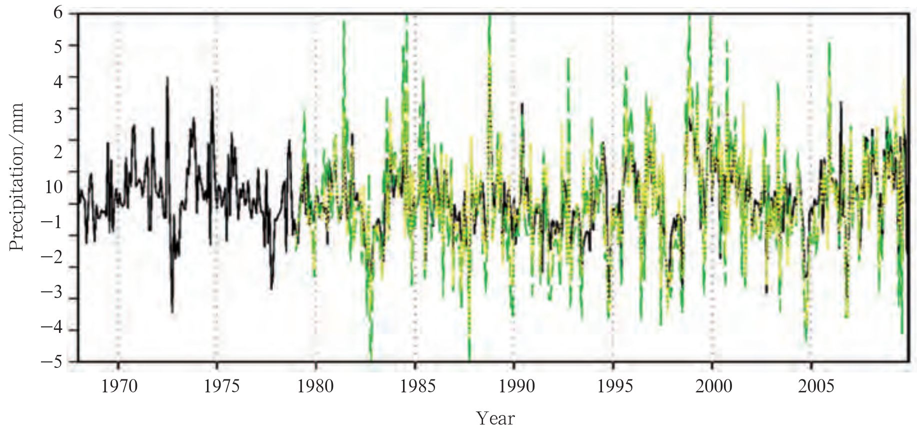

Fig.3. Time series of 5°–20°N, 105°–120°E average precipitation with climatology removed.

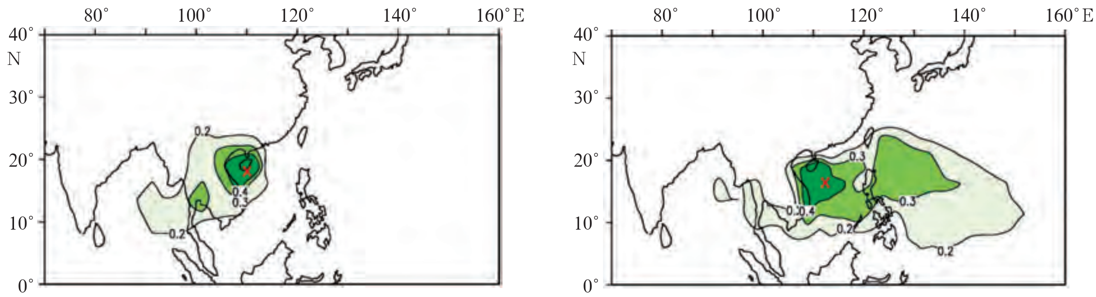

Fig.4. Correlations of Lingshui (18°30′N, 110°02′E) (a) and Xisha (16°50′N, 112°20′E) (b) station precipitation (mm) with NCEP precipitation. The cross marks denote location of stations.

than the CMAP and GPCP datasets (i.e., the NCEP precipitation has high correlation coefficients with the CMAP and the GPCP by values of 0.78 and 0.77, respectively). Moreover, Lingshui (18°30′N, 110°02′E) and Xisha (16°50′N, 112°20′E) are surface stations situated in the SCS. Figure 4 shows the correlation coefficients between the observed data and the NCEP precipitation. In the figure, we can find the highest positive correlations around the stations, indicating that the NCEP precipitation almost coincides with the observed data.

With an index of SCS 850 hPa southwesterly, it has been reported that the SCSSM exists in evident quasi-biennial variability (Zheng et al., 2009). In this paper, the SCSSM index defined as the average precipitation in the SCS also behaves with the quasi-biennial period (Fig. 5). Figure 5 displays two significant periods, namely, ≈57.6 and ≈28.8 months. Therefore, the time series of SCSSM TBO is established through the 18–36 months band-pass filtering precipitation in the SCS.

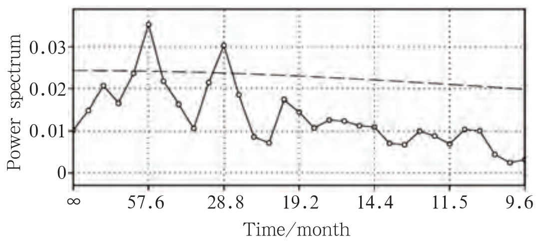

Fig.5. Power spectrum of 5°-20°N, 105°–120°E average precipitation. The long dash line denotes 95% significance level.

3 Air-sea interactions associated with SCSSM TBO

By computing the correlations between the time series of SCSSM TBO and lagged TBO filtering sea surface temperature anomalies (SSTAs) and surface wind anomalies, we obtained some connections of SSTAs and surface winds associated with the SCSSM TBO. In this paper, we use the abbreviations of MAM, JJA, SON and DJF to represent boreal spring (March-May), summer (June-August), autumn (September-November) and winter (December-next February), respectively. In this case, JJA(-1) means that the SSTAs and the surface wind anomalies lead 1a to the SCSSM TBO, i.e., calculating the correlations of SSTAs and surface wind anomalies for the previous JJA with the SCSSM TBO for the JJA. In addition, SON(-1), D(-1)JF(0), and MAM(0) represent 9, 6 and 3months leads, respectively, and JJA(0) denotes contemporary correlation.

3.1 *Seasonal cycle of SCSSM TBO*

In JJA(-1), the tropical WNP is a negative SSTA, while the tropical eastern-central Pacific (ECP) and Indian Ocean (IO) SSTs are positive anomalies (Fig. 6a). Tropical WNP negative SST anomalies form anomalous anticyclone in the SCS. Simultaneously, negative shearing vorticity over the SCS, with response to the tropical IO positive SSTAs, further strengthens the SCS anticyclonic anomalies. The anomalous anticyclone over the SCS restrains precipitation in this area, leading to less rainfall during the summer monsoon season. On the other hand, a weak convection in the SCS reduces cloud amount, so that more solar shortwave radiation reaches the sea surface, and the anticyclonic anomalies in this area form downwelling. Both increase SSTs (Fig. 6b). Meanwhile, there are northeasterly anomalies over the WNP, but at this time the background of the wind is southeasterly (Fig.2). On the basis of the evaporation-wind feedback mechanism, the SST increases in this area (Fig. 6b). The warm ECP enhances the convection in this area, which forms more clouds. This reduces shortwave radiations, which cool the SST in this region (Fig. 6b). Owing to the air-sea interactions mentioned above, the positive SSTAs in the SCS increase in SON(-1) and extend to the east of the Philippines, while the tropical ECP negative SST anomalies reduce and shrink to the central Pacific. This condition causes the anticyclonic anomalies to shift eastwards (Fig. 6b) as well. Thus, the cloud-SST negative feedback mechanism allows the warm SST in the tropical western Pacific to continue expanding eastwards, as the warm SST in the ECP maintains its cool temperature (Fig. 6c). In SON(-1) and D(-1)JF(0), there are northeasterly/southeasterly winds in the west of the central Pacific anomalous cyclone that are in the same direction as the trade winds. The evaporation-wind feedback mechanism also cools the SST of the tropical central Pacific. In addition, the trade winds drive the extra-tropical cold water and transport it to the equator, further reducing the eastern equatorial Pacific SST. From JJA(-1) to D(-1)JF(0), Australia is under the control of the anomalous anticyclone excited by the cold SST. There are further anomalous southeast flows over the Australian east coast, inducing an anomalous onshore current and downwelling that warm the

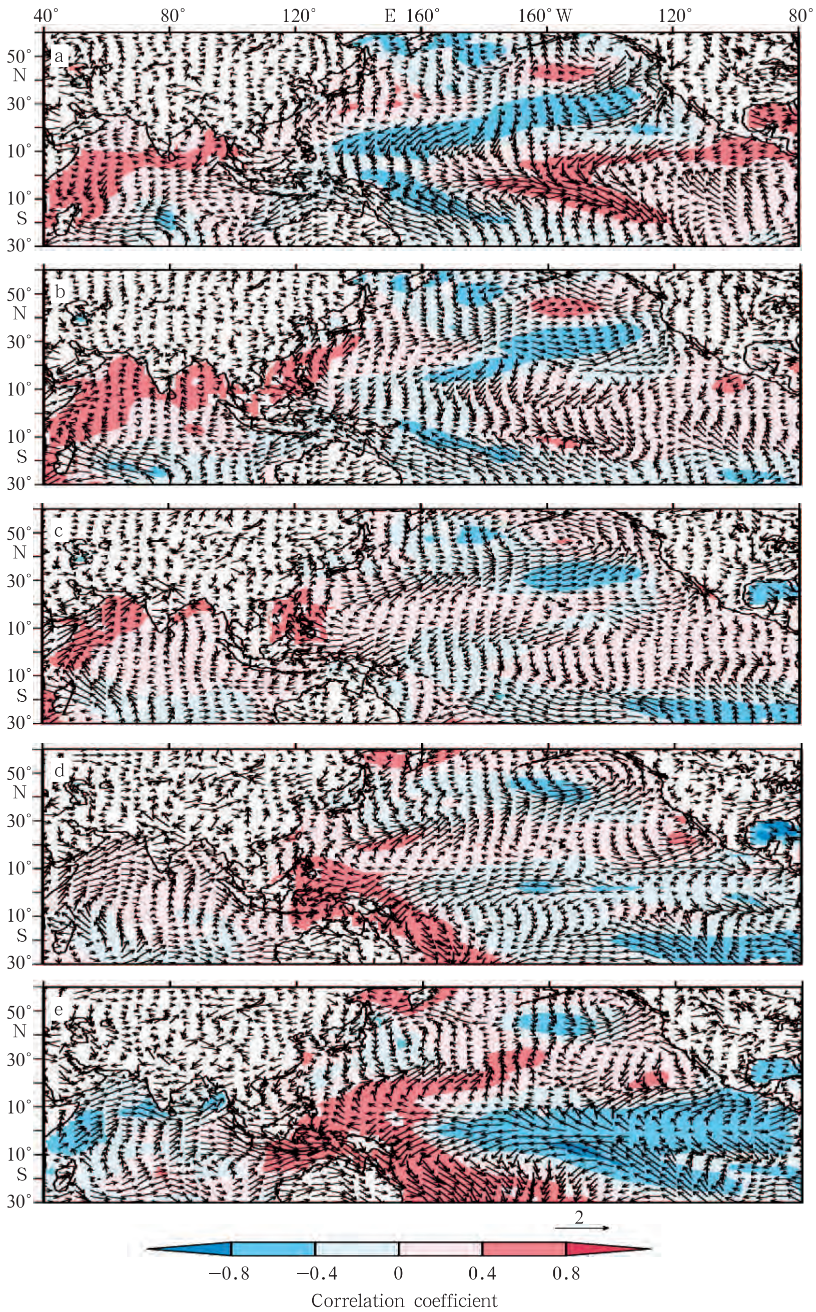

Fig.6. Lagged correlation coefficients of the TBO in SCSSM and SSTA (shadow) and surface winds (vectors) in JJA(-1) (a), SON(-1) (b), D(-1)JF(0) (c), MAM(0) (d) and JJA(0) (e), respectively. 0 means the reference year by SCSSM TBO, and -1 denotes the 1 a lead. More detailed descriptions can be seen in the text.

SST near the coast. In MAM(0), the warm SSTAs in the sea area on the east of Australia are very significant, whereas the tropical ECP is almost in the negative SSTAs (Fig. 6d). At this time, nearly all of the tropical Pacific Ocean is under the control of the anomalous anticyclone. Equatorial easterly anomalies strengthen the trade winds, further decreasing the equatorial SST (Fig. 6e). Thus, the half cycle of TBO in the SCS and the related air-sea interactions are completed.

3.2 *Effects of SCSSM TBO on tropical Indian Ocean and Pacific*

From Fig. 6, the SSTAs associated with the SCSSM TBO in the tropical ECP are significant, which tends into the extremum value in JJA before it decays. Evidently, the ECP SSTAs and the SCSSM TBO lock their phases in northern summer, that is, greatly different from the ENSO. Figure 7 shows the correlations of the TBO in the SCSSM with the Niño 3.4 SSTA and the western Pacific SSTA are the highest in JJA, decays in the SON, and develops in the MAM. On the contrary, the correlation of the

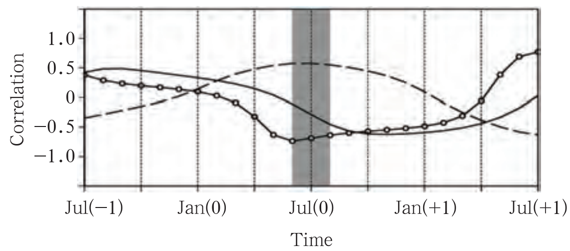

Fig.7. Lagged correlations between the SCSSM TBO and Niño 3.4 SSTA (open cycle line), western equatorial Pacific (dash line, 5° S–5°N, 120°–160°E), and north Indian Ocean (solid line, 0°–15°N, 40°–100°E). The shaded area represents the season of the SCSSM in the reference year. The values –1, 0, and +1 denote last, present and next year, respectively.

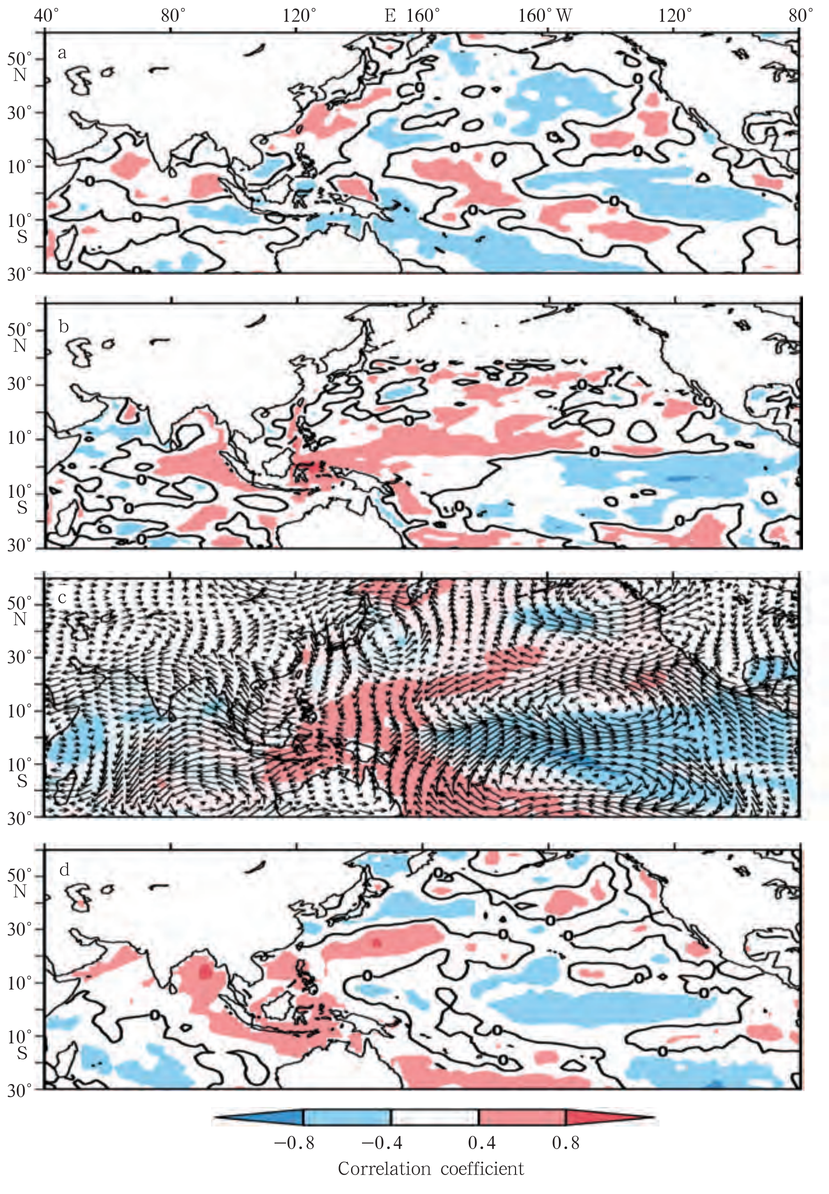

Fig.8. Correlation coefficients of the SCSSM with latent heat flux (a), thermocline depth (b), 200 hPa winds and SSTAs (c), and net short-wave radiation (d) on the quasi-biennial scale.

TBO and the western equatorial IO is the highest in the SON, decreases in the DJF and the MAM, and develops in the JJA. In particular, the SSTA signal associated with the SCSSM TBO is nearly impossible to find in the Niño 3.4 region during the D(-1)JF(0); however it is significant in the D(0)JF(+1) to some extent. This implies that on the quasi-biennial scale, SCSSM may affect the ENSO rather than be affected by it.

Why does the seasonal SSTA evolution in the tropical Pacific associated with the SCSSM TBO has a phase-lock in the JJA? This can be attributed to ocean-atmosphere coupled processes; in fact, the pattern shown in Fig. 6e can be maintained and strengthened through the air-sea interactions. When the SCSSM is strong, there are two anomalous transverse circulations responses in the tropical IO and Pacific as well as descending branches located at the western equatorial IO and the equatorial ECP, respectively.

First, we explore the tropical IO. In the JJA, southwesterly winds prevail in the north IO and are consistent with the anomalous winds (Fig. 6e), causing more upward latent heat flux (Fig. 8a) and decreased the SST. Oceanic offshore currents are formed due to anomalous alongshore flows, and then upwelling and induced the shallow thermocline (Fig. 8b) can reduce the SST. In addition, the anomalous latent heat flux and the westerly winds enhance the Indian summer monsoon and increase the cloud amount, which reduces the shortwave radiation and then cools the SST. Simultaneously, the anomalous cold SST can lead to more descending flows to strengthen the western transverse circulation, thus enhancing the convection over the SCS. This is a positive feedback.

On the other hand, descending flows over the equatorial ECP can reduce the cloud amount and allow more solar shortwaves to come into the ocean to warm the SST (Fig. 8d). In addition, induced anomalous cold source in the mid-troposphere excites two anomalous low-level anticyclones located in its western region (Fig. 6e) as well as two anomalous cyclones in the high level (Fig. 8c). Low-level anticyclones can cause the Ekman convergence in the oceanic boundary layer to deepen the thermocline (Fig. 8b). Over the southwest and eastern equatorial Pacific, the anomalous winds have opposite signs with the mean flow, and as such, evaporation-wind feedback mechanism can increase the SST (Fig. 8a). Moreover, winds inducing the oceanic onshore currents lead to deeper thermocline and warm the SST in the southwest Pacific to the east of Australia (Fig. 8b). Over the western equatorial Pacific, including the east of maritime continent, there are anomalous winds against the mean flow; thus, evaporation-wind feedback mechanism can also increase the SST.

As low-level divergence induced wind stress leads to upwelling in the tropical ECP, the thermocline tends to be shallow (Fig. 8b) and the SST would decrease. Moreover, a more prominent Rossby wave in the Southern Hemisphere is noticeable because of the east transverse circulation of descending branch equatorial asymmetry located somewhat south to the equator. Although the anomalous southeasterly winds have the same directions as the trades in the west of the southeastern Pacific, evaporation-wind feedback mechanism also makes the SST cooler. Hence, the resulting-enhanced descending flows strengthen the east transverse circulation to strengthen the con-

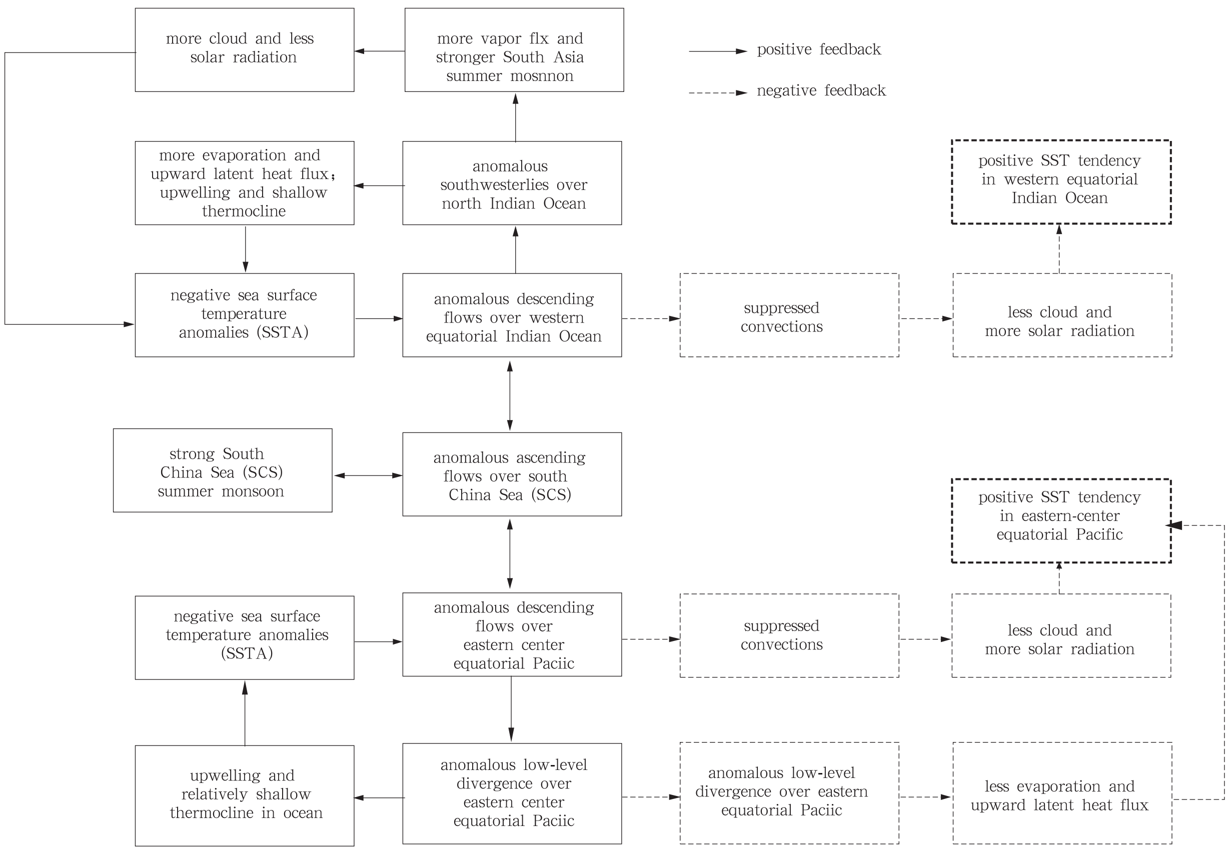

Fig.9. Air-sea interactive physical processes related with the SCSSM TBO.

vection in the SCS. This is a positive feedback process as well.

4 Conclusions and discussion

There are air-sea interactions associated with the SCSSM TBO both in the tropical IO and the Pacific. Particularly, the SSTAs of the tropical northern IO and the ECP have their respective positive feedback processes with the SCSSM on the quasi-biennial time scale, as shown in Fig. 9. For the north IO, several positive feedback processes are aggregated in the JJA(0), except a negative feedback in the western equatorial IO. Thus, the resulted whole northern IO SST tends to be cool in the JJA(0). By the SON(0), the central convection moves to the maritime continent, after which the west transverse circulation is composed of the descending flows in the western north IO and the ascending flows in the maritime continent. As the north IO becomes cold overall in the JJA(0), the induced weak convection and fewer amounts of cloud allow more solar radiation to go into the sea, thus warming the SST. However, at the same time, evaporation-wind feedback and a shallow thermocline induced by the anomalous alongshore winds cool the SST. Therefore, some balance is met, and the SSTA comes into the extremum in the SON(0). On the contrary, a balance should be met in the ECP in the JJA(0) with one positive and two negative feedback processes (Fig. 9). As a result, the equatorial ECP SSTA associated with the SCSSM TBO reaches its extreme the in JJA(0), that is, greatly different from the ENSO. The convection shifts to the maritime continent in the SON(0); meanwhile, the descending branch moves to the southeastern Pacific, thus weakening the anomalous descending flows in the equatorial ECP. At this time, the negative feedback processes dominate the change of the equatorial ECP SST, although the negative SSTA can nearly persist throughout SON(0), even D(0)JF(1) (the figure omitted). This is the reason why the Niño 3.4 SSTA associated with the SCSSM TBO reaches the extremum in the JJA(0), while the north IO reaches the SSTA in SON(0). Since the ECP SSTAs associated with the SCSSM TBO have mature phase in boreal summer, it implies that on the quasi-biennial scale, the SCSSM may affect the ENSO rather than be affected by it.

In addition to the equatorial ECP contribution, the north IO SSTA may play an important role in the TBO in the SCSSM as well (see Fig. 6). Nonetheless, why is the descending branch of the east transverse circulation located at the south of the equator in the JJA(0)? A possible cause is the north bias of the ITCZ over the ECP, which leads to the south bias of the descending flows relative to the equator in the JJA(0). Further studies are required to explore the possible reasons behind this phenomenon.

References

Carton J A, Chepurin G, Cao X, et al. 2000a. A simple ocean data assimilation analysis of the global upper ocean 1950–1995: Part 1. Methodology. J Phys Oceanogr, 30(2): 294–309

Carton J A, Chepurin G, Cao X. 2000b. A simple ocean data assimilation analysis of the global upper ocean 1950–1995: Part 2. Results. J Phys Oceanogr, 30(2): 311–326

Chen M, Xie P, Janowiak J E, et al. 2002. Global land precipitation: a 50-yr monthly analysis based on gauge observations. J Hydrometeorology, 3(3): 249–266

Ding Yihui, Li Chongyin, Liu Yanju. 2004. Overview of the South China Sea monsoon experiment (SCSMEX). Adv Atmos Sci, 21(3): 1–18

Huang R H, Sun F Y. 1992. Impact of the tropical western Pacific on the East Asian summer monsoon. J Meteor Soc Japan, 70(1B): 243–256

Kalnay E, Kanamitsu M, Kistler R, et al. 1996. The NCEP/NCAR 40-year reanalysis project. Bulletin of the American Meteorological Society, 77(3): 437–472

Kurihara K. 1989. A climatological study on the relationship between the Japanese summer weather and the subtropical high in the western North Pacific. Geophysical Magazine, 43(2): 45–104

Lau, K M, Ding Y, Wang J-T, et al. 2000. A report of the field operations and early results of the South China Sea monsoon experiment (SCSMEX). Bull Am Meteorol Soc, 81(6): 1261–1270

Li T, Wang B. 2005. A review on the western North Pacific monsoon: synoptic-to-interannual variability. Terrestrial, Atmospheric and Oceanic Sciences, 16(2): 285–314

Lu R. 2001. Interannual variability of the summertime North Pacific subtropical high and its relation to atmospheric convection over the warm pool. J Meteor Soc Japan, 79(3): 771–783

Nitta T. 1987. Convective activities in the tropical western Pacific and their impact on the northern hemisphere summer circulation. J Meteor Soc Japan, 65(3): 373–390

Smith T M, Reynolds R W, Peterson T C, et al. 2008. Improvements to NOAA's historical merged land-ocean surface temperature analysis (1880–2006). J Climate, 21(10): 2283–2296

Tao S Y, Chen L X. 1987. A review of recent research on the East Asia summer monsoon in China. In: Chang C P, Krishnamurti T N, Eds. Monsoon Meteorology. Oxford: Oxford University Press, 60–92

Wang B, Huang F, Wu Z, et al. 2009. Multi-scale climate variability of the South China Sea monsoon: a review. Dynamics of Atmospheres and Oceans, 47(1–3): 15–37

Wang B, Lin H. 2002. Rainy seasons of the Asian-Pacific monsoon. J Climate, 15(4): 386–398

Wang C, Wang W, Wang D, et al. 2006. Interannual variability of the South China Sea associated with El Niño. J Geophys Res, 111, C03023, doi:10.1029/2005JC003333

Wang B, Wu R, Fu X. 2000. Pacific-East Asian teleconnection: how does ENSO affect East Asian climate? J Climate, 13(9): 1517–1536

Wang B, Wu R, Lau K-M. 2001. Interannual variability of Asian summer monsoon: contrast between the Indian and western North Pacific-East Asian monsoons. J Climate, 14(20): 4073–4090

Wang Dongxiao, Xie Qiang, Du Yan, et al. 2002. The 1997-1998 warm event in the South China Sea. Chinese Science Bulletin, 47(14): 1221–1227

Wang B, Zhang Q. 2002. Pacific-East Asian teleconnection: Part II. How the Philippine Sea anticyclone established during development of El Niño. J Climate, 15(22): 3252–3265

Zeng L, Shi P, Liu W T, et al. 2009. Evaluation of a satellite-derived latent heat flux product in the South China Sea: a comparison with moored buoy data and various products. Atmospheric Research, 94(1): 91–105

Zeng L, Wang D. 2009. Intraseasonal variability of latent-heat flux in the South China Sea. Theoretical and Applied Climatology, 97(1–2): 53–64

Zheng Bin, Li Chunhui, Lin Ailan, et al. 2009. Features and comparisons of the quasi-biennial variations in the Asia-Pacific monsoon subsystems. Journal of Tropical Meteorology, 15(1): 116–120